

Nickel(II) complexes bearing phosphinooxazoline ligands: Synthesis, structures and their ethylene oligomerization behaviors

Xiubo Tang^a, Dongheng Zhang^a, Suyun Jie^a, Wen-Hua Sun^{a,*}, Jiutong Chen^b

^a Key Laboratory of Engineering Plastics, Institute of Chemistry, Chinese Academy of Sciences, Beijing 100080, China

^b State Key Laboratory of Structural Chemistry, Fujian Institute of Research on the Structure of Matter, Chinese Academy of Sciences, Fuzhou 350002, China

Received 26 January 2005; received in revised form 12 May 2005; accepted 24 May 2005

Available online 24 June 2005

Abstract

A series of Ni(II) complexes **4a–f** ligated by the unsymmetrical phosphino-oxazolines (PHOX) were synthesized and characterized by elemental analysis and IR spectroscopy, and the structures of complexes **4c–4e** were confirmed by the X-ray crystallographic analysis. All derivatives showed distorted tetrahedron geometry by the nickel center and coordinative atoms. Upon activation with methylaluminoxane (MAO) or Et₂AlCl, these complexes exhibited considerable to high activity of ethylene oligomerization. The ligands environments and reaction conditions significantly affect their catalytic activities, while the highest oligomerization activity (up to $1.18 \times 10^6 \text{ g} \cdot \text{mol}^{-1}(\text{Ni}) \cdot \text{h}^{-1}$) was observed for **4d** at 20 atm of ethylene. Incorporation of 2–4 equivalents of PPh₃ as auxiliary ligands in the **4a–f**/MAO catalytic systems led to higher activity and longer catalytic lifetime.

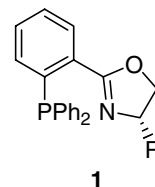
© 2005 Elsevier B.V. All rights reserved.

Keywords: Phosphinooxazoline ligand; Nickel complex; Ethylene oligomerization

1. Introduction

The ethylene oligomerization represents a major industrial process for the production of linear α -olefins, which are extensively used in the preparation of detergents, plasticizers, fine chemicals as well as monomers for copolymerization with ethylene in the production of the linear low-density polyethylene (LLDPE). The linear α -olefins were originally manufactured by the Ziegler (Alfen) process [1], and current industrial catalysts include either alkylaluminum compound or a combination of alkylaluminum compound with early transition metal compounds or nickel (II) complexes containing bidentate monoanionic [P,O] ligands (the SHOP process) [2]. The discovery of the cationic (diimino NiCl₂) complexes [3] as effective catalysts for ethylene oligomerization and polymerization

resurrected the interest in designing new catalysts of late-transition metal complexes with various ligands, such as, diimine [4], unsymmetrical pyridylimine [5], salicylaldimine [6] and phosphine-containing ligands [7]. These numerous studies enrich the knowledge about the effects of the ligand backbone on the catalysis behavior or mechanism aspect of the catalyzing process, although only a few examples of the catalysts are comparable to Brookhart's diimine–Ni(II) complexes in the catalytic activity [8].



a R = Bn **d** R = *t*-Bu
b R = *i*-Pr **e** R = Me
c R = Ph

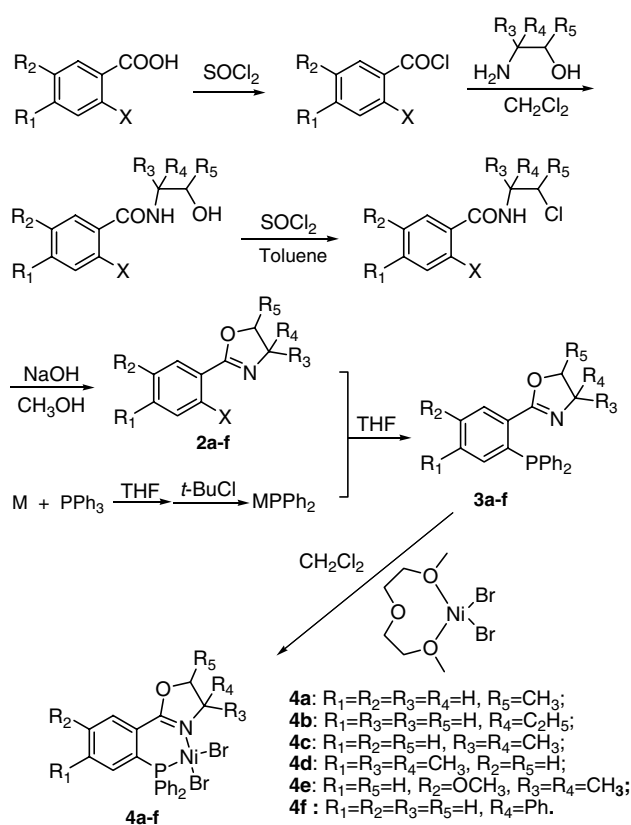
* Corresponding author. Tel.: +86 1062557955; fax: +86 1062618239.
E-mail address: whsun@iccas.ac.cn (W.-H. Sun).

The chiral phosphino-oxazoline (PHOX) ligands **1**, first developed independently in 1993 by Pfaltz, Helmchen, and Williams as highly effective non- C_2 -symmetric ligands for asymmetric allylic alkylation, have been applied with great success in a diverse range of asymmetric catalytic reactions [9]. Moreover, it would be interesting to explore the scope of their coordination with late-transition metals and their further application in catalytic systems. In our screening new nickel complexes ligated by [P,N] ligands for ethylene oligomerization, a series of various PHOX ligands could provide the information of stereo- bulky and electronic effects around nickel center and their relationship to the catalytic activities because the adaptation of substituents on oxazoline are promising. Therefore we designed and synthesized a series of Ni(II) complexes ligated by various PHOX and investigated the catalytic behaviors of the nickel complexes upon activation of methylaluminoxane (MAO) or Et_2AlCl as well as the presence of PPh_3 as auxiliary ligand. Herein we report the synthesis and characterization of a series of (PHOX)NiBr₂ complexes and their catalytic behaviors in ethylene oligomerization.

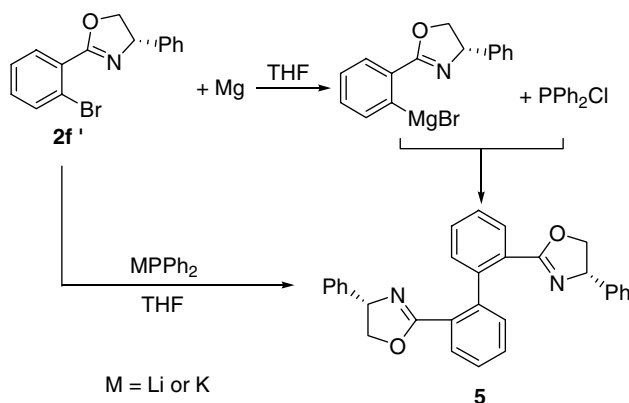
2. Results and discussion

2.1. Synthesis of the PHOX ligands **3a–f**

The 2-(2-bromophenyl)-oxazoline **2a–e** and 2-(2-fluorophenyl)-oxazoline **2f** were prepared in high yield according to the methods cited in the literature [10]. **2a–f** were characterized by elemental analysis and ¹H NMR spectroscopy. The bromo-substituted precursors **2a–e** can react with LiPPh₂ in THF to furnish the PHOX ligands **3a–e** in acceptable yields (Scheme 1). While for the synthesis of the ligand **3f**, when the bromo-substituted precursor to compound **5** was obtained as the dominant product, along with a trace of ligand **3f**. Synthesis via the Grignard reagent procedure also furnished the compound **5** as the main product (Scheme 2). Therefore, we employed the 2-(2-fluorophenyl)-oxazoline **2f** as precursor to react with the phosphine reagent KPPH₂ in refluxing THF [11], and fortunately, the ligand **3f** was obtained in good yield, though the homo-coupling reaction could not be completely avoided. The racemic ligands **3a** and **3b** were obtained from the racemic starting materials, while the chiral ligand **3f** was synthesized using (S)-(+)-2-amino-2-phenylethanol and 2-fluorobenzoic acid as starting materials. These ligands were isolated as colorless oil or white solid by flash column chromatography. Slow oxidation of the ligands occurred when they are exposed to air. Ligands **3a–f** were characterized by elemental analysis, ¹H NMR, ³¹P NMR and IR spectroscopy. The ¹H NMR spectrum



Scheme 1. Synthesis of the complexes **4a–4f**. For **3a–e**, X = Br, M = Li; for **3f**, X = F, M = K.



Scheme 2. Synthesis of the compound **5**.

of ligand **3a**, in which the 5-position (neighboring the oxygen atom) of the oxazoline ring is substituted by one methyl group, contains one triplet and one quadruplet at 3.70 and 4.18 ppm, respectively, which are assignable for the CH₂ protons in 4-position of the oxazoline ring. The separation of chemical shifts for the two protons attached to the same carbon is due to their inequivalent chemical environment. One proton is in *cis*-conformation to the methyl group in the vicinal

carbon, while another proton is in *trans*-conformation to this substituent. Similar effect is also observed in the ^1H NMR spectra of **3b** and **3f**.

2.2. Synthesis of the complexes **4a–f**

The Ni(II) complexes **4a–f** were prepared by stirring the corresponding ligands with 0.95 equiv of nickel(II) bromide 2-methoxyethyl ether [(MEE)NiBr₂] for 10 h in dichloromethane at 25 °C. After workup, the Ni(II) complexes were isolated as air-stable orange or purple powder in 67–90% yields.

These complexes were characterized by IR spectral and elemental analysis. The elemental analysis reveals that the components of these complexes are in accordance with the formula MLBr₂. In the IR spectra, the stretching vibration of $\nu_{\text{C}=\text{N}}$ in complexes show red shifts by 20–40 cm⁻¹ with remarkable decrease in intensity in comparison to the corresponding ligands, which indicates the coordination of the nitrogen atom in the oxazoline ring to the metal center. The paramagnetic nature of these complexes hinders their NMR characterization.

The single crystals of **4c–4e** suitable for X-ray crystallography were grown by layer-diffusion of hexane into their dichloromethane solutions. The molecular structures of **4c–4e** are depicted in Figs. 1–3, respectively. Their selected bond lengths and angles are listed in Table 1. The coordination geometry around the nickel centers for complexes **4c–4e** are similar and all adopt distorted tetrahedron. Hence, only the crystal structure of **4c** was selected to describe in detail. The P, N bite angle (P(1)–Ni(1)–N(1), 89.32(10)°) in **4c** is comparable to the recently reported P–Ni–N angle (83.52(9)°) of the square planar [NiCl₂(P, N)]-type complex [7e] and remarkably deviates from the ideal tetrahedron. The P(1)–Ni(1) and N(1)–Ni(1) bond lengths are also similar to the previously reported values [7e,12]. The C(7)–N(1) bond length in the oxazoline ring has distinctive double-

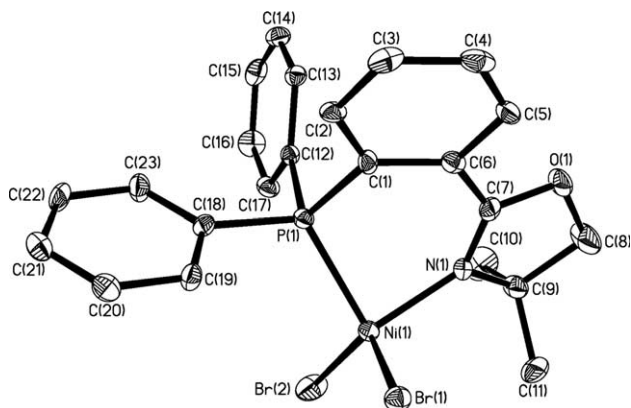


Fig. 1. Molecular structure of **4c**. Hydrogen atoms and CH₂Cl₂ are omitted for clarity.

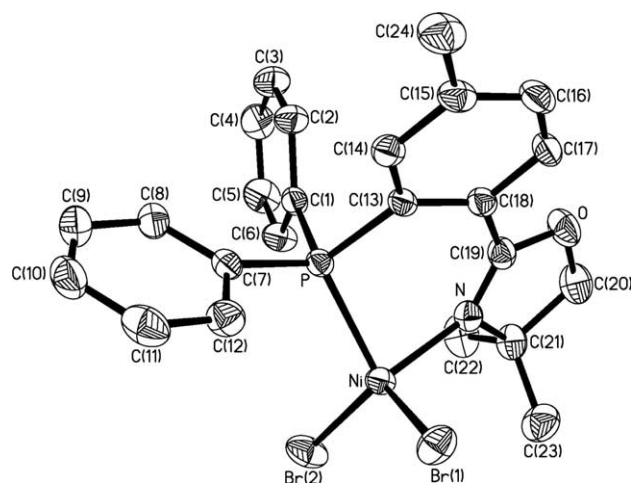


Fig. 2. Molecular structure of **4d**. Hydrogen atoms are omitted for clarity.

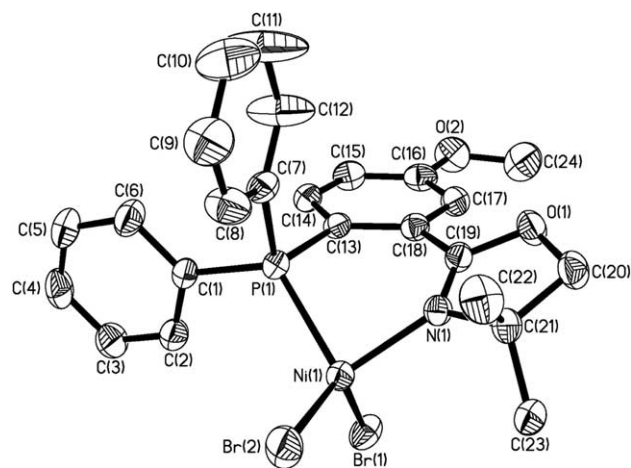


Fig. 3. Molecular structure of complex **4e**. Hydrogen atoms are omitted for clarity.

bond character with the bond length of 1.299(5) Å. The N(1), Ni(1), P(1), C(1), C(6) and C(7) atoms in the chelate ring are nearly coplanar and the mean deviation from the plane is 0.2673 Å. In addition, the oxazoline ring and the coordination ring are approximately coplanar with a dihedral angle of 15.4°, and therefore, the two methyl groups attached to C(9) may provide some steric hindrance on the axial sites. In addition, the geometry around phosphine is also distorted tetrahedral with angles in the range of 104.5(2)–117.95(14) and the three phenyl rings attached to the phosphine atom are roughly perpendicular to each other with the dihedral angles of 73.2°, 84.3° and 92.5°, respectively.

2.3. Catalytic oligomerization of ethylene

These nickel(II) complexes were investigated in the oligomerization of ethylene using MAO or AlEt₂Cl as cocatalyst, and the results are listed in Table 2. In all

Table 1
Selected bond lengths and bond angles for complex **4c–4e**

4c		4d		4e	
<i>Bond lengths (Å)</i>					
Ni(1)–N(1)	1.975(3)	Ni–N	1.9900(19)	Ni(1)–N(1)	1.983(2)
Ni(1)–P(1)	2.2637(12)	Ni–P	2.2731(6)	Ni(1)–P(1)	2.2740(9)
Ni(1)–Br(1)	2.3687(9)	Ni–Br(1)	2.3595(5)	Ni(1)–Br(1)	2.3710(6)
Ni(1)–Br(2)	2.3236(9)	Ni–Br(2)	2.3303(4)	Ni(1)–Br(2)	2.3288(5)
P(1)–C(1)	1.816(4)	P–C(7)	1.814(2)	P(1)–C(1)	1.814(3)
P(1)–C(12)	1.809(4)	P–C(1)	1.817(2)	P(1)–C(7)	1.820(3)
P(1)–C(18)	1.816(4)	P–C(13)	1.827(2)	P(1)–C(13)	1.821(3)
<i>Bond angles (°)</i>					
N(1)–Ni(1)–P(1)	89.32(10)	N–Ni–P	88.49(6)	N(1)–Ni(1)–P(1)	88.09(7)
N(1)–Ni(1)–Br(1)	101.63(10)	N–Ni–Br(1)	104.40(6)	N(1)–Ni(1)–Br(1)	100.19(7)
N(1)–Ni(1)–Br(2)	120.81(10)	N–Ni–Br(2)	118.62(6)	N(1)–Ni(1)–Br(2)	119.27(7)
P(1)–Ni(1)–Br(1)	104.30(5)	P–Ni–Br(1)	103.73(2)	P(1)–Ni(1)–Br(1)	104.54(2)
P(1)–Ni(1)–Br(2)	110.40(4)	P–Ni–Br(2)	114.67(2)	P(1)–Ni(1)–Br(2)	113.67(3)
Br(1)–Ni(1)–Br(2)	124.05(3)	Br(1)–Ni–Br(2)	121.338(17)	Br(1)–Ni(1)–Br(2)	124.40(2)
C(1)–P(1)–C(12)	105.50(18)	C(1)–P–C(7)	106.84(10)	C(1)–P(1)–C(7)	105.39(13)
C(1)–P(1)–C(18)	105.72(19)	C(1)–P–C(13)	103.56(10)	C(1)–P(1)–C(13)	105.41(13)
C(12)–P(1)–C(18)	104.5(2)	C(7)–P–C(13)	106.90(10)	C(7)–P(1)–C(13)	106.22(13)
C(1)–P(1)–Ni(1)	104.61(14)	C(1)–P–Ni	114.10(8)	C(1)–P(1)–Ni(1)	119.64(10)
C(12)–P(1)–Ni(1)	117.32(13)	C(7)–P–Ni	119.46(8)	C(7)–P(1)–Ni(1)	115.11(10)
C(18)–P(1)–Ni(1)	117.95(14)	C(13)–P–Ni	104.57(7)	C(13)–P(1)–Ni(1)	103.92(9)

Table 2
Ethylene oligomerization with **4a–f** at 1 atm of ethylene^a

Entry	Complex	Al/Ni (mol)	Temp (°C)	Time (min)	Activity ^b 10 ⁵ g · mol ⁻¹ (Ni) · h ⁻¹	Oligomers distribution ^b (%)			
						C ₄ /ΣC	C ₆ /ΣC	C _{≥8} /ΣC	Linear α-olefin
1	4a	1000	25	30	2.29	89.62	10.38	–	11.0
2	4b	1000	25	30	0.71	99.38	0.62	–	52.6
3	4c	1000	25	30	1.78	85.50	11.59	2.91	33.1
4	4d	1000	25	30	3.73	75.72	21.94	2.34	19.5
5	4e	1000	25	30	3.95	84.13	14.79	1.09	25.41
6	4f	1000	25	30	1.34	82.40	14.47	3.13	21.29
7	4c	500	25	30	1.46	88.93	6.62	4.45	22.7
8	4c	1500	25	30	1.10	95.45	4.55	–	22.9
9	4c	1000	0	30	1.08	98.20	1.80	–	32.2
10	4c	1000	40	30	0.54	98.48	1.52	–	52.2
11	4c	1000	25	60	0.98	81.77	14.79	3.42	23.6
12	4c	1000	25	90	0.60	81.88	15.70	2.49	15.8
13 ^c	4c	20	25	30	0.60	98.54	1.46	–	9.63
14 ^c	4c	50	25	30	6.66	74.21	18.40	7.39	8.5
15 ^c	4c	100	25	30	2.72	80.71	12.61	6.67	17.84

^a General conditions: 5 μmol precatalyst; 30 mL toluene as solvent; MAO as cocatalyst.

^b Determined by GC, ΣC means the total amounts of oligomers.

^c AlEt₂Cl as cocatalyst.

the cases, ethylene dimers and trimers are the main oligomeric products. As analyzed by GC and GC-MS, the selectivities for α-olefins in total olefins are relatively lower.

2.3.1. The effect of ligand environment on the ethylene oligomerization behaviors

It is observed that the size and position of the substituents in the ligand backbone of the catalysts slightly affect their ethylene oligomerization activity. Among complexes **4a–4c**, **4a** with a methyl substituent in the

5-position of the oxazoline ring shows the highest activity under identical reaction conditions. In comparison, **4b** with an ethyl group in the 4-position of the oxazoline ring shows the lowest activity (entry 1–3, Table 2). On comparing the structures of **4a** and **4b**, it can be observed that the ethyl substituent in the 4-position of the oxazoline ring is closer to the nickel and will provide the steric shielding around the metal center. In addition, substitution in the *ortho* position of the coordinated nitrogen with electron-donating ethyl group will result in a lower positive charge on nickel of the active catalytic species

and, subsequently, weakens the metal–ethylene interaction during the ethylene oligomerization. However, methyl group in the 5-position of the oxazoline ring is too far away from the metal center to affect its electronic properties. Due to the steric and electronic considerations, it is easily understood that complex **4b** displays lower ethylene oligomerization activity than its counterpart **4a**. However, their oligomerization activities increase obviously when the ligand has a substituent on the phenyl ring attached to the oxazoline, either methyl (**4d**) or methoxyl (**4e**), compared to the analogue **4c**. The previous studies about the electronic effects on the ethylene polymerization activity gave the inconsistent results. It is a general notion that decrease in the donor ability of the substituents, (i.e. increase in the electrophilicity of the metal center) should decrease the insertion barrier, thus, resulting in higher activity [13]. While some of the experimental [7a] and theoretical [14] results show that in square-planar *d* [8] transition-metal complexes containing unsymmetrical bidentate ligands and methyl ethylene, increasing the donor strength *trans* to the strong donor methyl group should lower the migration barrier, while decreasing the donor strength should raise the insertion barrier. In complex **4f**, the bulky phenyl ring was introduced to the 4-position of the oxazoline, which will exert efficient steric hindrance to the metal center. However, the electron-withdrawing property of the phenyl ring will result in the formation of a more electrophilic active catalytic metal center. Due to these combined steric and electronic effects, the oligomerization activity of **4f** is higher than that of **4b** and is lower than that of **4a**. In all the cases, the dimer and trimer of ethylene are the major products. The selectivity for ethylene dimer of **4b** is especially high to 99.38%. Complex **4d** shows the trend to produce oligomers with higher carbon number. However, the lower oligomers (C₄ and C₆) as major products will be not interested in industrial consideration, moreover, the intern olefins are not pursued in ethylene oligomerization. In general, the effects of the ligand environment on the distribution of oligo-

mers are not as obvious as the catalytic activities for the oligomers.

2.3.2. The effect of reaction parameters on the ethylene catalytic activities

To probe the effect of reaction parameters on the ethylene oligomerization behaviors, the precatalyst **4c** was typically investigated via changing the amounts of MAO, the reaction temperature and the reaction time.

Variation of the Al/Ni molar ratio in the range of 500–1500 shows insignificant effect on oligomerization activities and oligomer distributions, although the highest oligomerization activity was observed when the Al/Ni molar ratio is 1000. The catalyst **4c** shows higher oligomerization activity at lower temperature, and elevating the reaction temperature to 40 °C leads to the remarkable reduction in activity (entry 10, Table 2), which may be ascribed to the decomposition of the active catalytic sites and lower ethylene solubility at higher temperature. The oligomerization activities progressively decrease when reaction was prolonged from 30 to 60 min and finally to 90 min, which indicates that the catalyst lifetime is relative short. Recently Braunstein group reported that their $\dot{N}P$ coordinated nickel complexes show high ethylene oligomerization activity upon activation with only slightly excess of AlEtCl₂ [7d,7e,7f], and we tested the ethylene oligomerization with complex **4c** using AlEt₂Cl instead of MAO as cocatalyst. It is observed that the complex **4c** displays high activity with only 50 equivalents of AlEt₂Cl as cocatalyst (entry 14, Table 2).

2.3.3. The effects of the ethylene pressure on the oligomerization behavior

The complexes **4a–f** were also tested for ethylene oligomerization at 20 atm of ethylene pressure and the results are summarized in Table 3. The results show that increase in the ethylene pressure lead to the remarkable increase in ethylene activity. This observation of the increased oligomerization activity at the elevated ethylene pressure

Table 3
Ethylene oligomerization with **4a–f**/MAO at 20 atm of ethylene^a

Entry	Complex	Activity ^b 10 ⁵ g · mol ⁻¹ Ni · h ⁻¹	Oligomers distribution ^b (%)			
			C ₄ /ΣC	C ₆ /ΣC	C _{≥8} /ΣC	Linear α-olefin
1	4a	5.74	78.90	7.84	13.26	13.8
2	4b	5.42	45.47	7.24	47.29	28.6
3 ^c	4c	6.27	79.06	7.63	13.31	30.4
4	4d	11.80	85.34	9.31	5.35	23.1
5	4e	7.37	82.07	6.63	11.30	17.4
6	4f	7.99	90.21	4.36	5.43	16.8

^a General conditions: 20 μmol catalyst; 150 mL toluene; Al/Ni = 1000; 25 °C; 30 min.

^b Determined by GC, ΣC means the total amounts of oligomers.

^c Determined by GC-MS.

Table 4
Ethylene oligomerization with **4a–f**/MAO at 1 atm in the presence of PPh₃^a

Entry	Complex	Al/Ni/PPh ₃ (mol)	Time (min)	Activity ^b 10 ⁵ g · mol ⁻¹ Ni · h ⁻¹	Oligomers distribution ^b (%)			
					C ₄ /ΣC	C ₆ /ΣC	C _{≥8} /ΣC	Linear α-olefin
1	4a	1000:1:2	30	5.27	88.90	10.79	0.3	6.2
2	4b	1000:1:2	30	2.71	91.00	5.91	3.09	12.1
3	4c	1000:1:2	30	2.62	78.70	20.05	1.25	4.7
4	4d	1000:1:2	30	3.62	91.13	7.30	1.57	7.9
5	4e	1000:1:2	30	4.40	77.12	21.36	1.52	6.3
6	4f	1000:1:2	30	11.20	79.32	19.01	1.67	8.30
7	4c	200:1:2	30	1.73	90.67	9.33	–	12.4
8	4c	500:1:2	30	3.76	77.87	21.70	0.43	4.4
9	4c	500:1:4	30	4.05	82.80	16.95	0.25	9.0
10	4c	500:1:10	30	1.40	89.73	10.27	–	11.7
11	4c	500:1:2	60	3.33	71.60	25.62	2.78	2.3
12	4c	500:1:2	90	2.44	76.70	22.33	0.97	5.5

^a General conditions: 5 μmol precatalyst; 30 mL toluene as solvent; 25 °C.

^b Determined by GC, ΣC means the total amounts of oligomers.

is in accordance with the previously reported results for the homogenous nickel catalyst [15]. At 20 atm of ethylene pressure, the effect of the ligand environments on the oligomerization activity is similar to the results of 1 atm. In addition, the percentages of the higher carbon number olefins in the oligomeric product are much higher than the runs at 1 atm of ethylene pressure. No significant improvement of the selectivity for α-olefin was observed at the elevated ethylene pressure.

2.3.4. The effect of auxiliary ligand (PPh₃) on ethylene oligomerization behaviors

For catalyst precursors **4a–f**, oligomerization activities were remarkably enhanced when PPh₃ was used as the auxiliary ligand, and the results are listed in Table 4. Similar effect of PPh₃ was also observed in our recent investigation on pyridine-monoimine Ni(II)/MAO catalyst system [5d]. Contrarily, the decrease of ethylene polymerization activity was also reported as due to the addition of 5 equiv of PPh₃ for the neutral nickel (II) catalyst [16]. GC analysis indicates that the oligomer distributions are not remarkably affected by the presence of PPh₃ in the reaction system and the selectivity for 1-butene is still very low in the presence of PPh₃ as auxiliary ligand. Results on the oligomerization reactivity with various Ni/PPh₃ molar ratio for **4c** show that 2–4 equiv of PPh₃ is optimal for accelerating the oligomerization reaction, and increase the PPh₃ amount to 10 equiv leads to the reduction in oligomerization activity (entries 7–9, Table 4). In addition, less amount of MAO is sufficient for activation of the precatalyst to reach the highest value. The turnover number (TON) keeps increasing when the reaction time is increased from 30 to 90 min (4700, 11,900 and 13,100 for 30, 60 and 90 min, respectively), which indicates that part of the active catalytic species are still alive after 60 min. The longer reaction time produced higher order oligo-

mers on the base of entries of 7, 11 and 12 in Table 2 because of further propagation of ethylene insertion.

The mechanism of the acceleration phenomena of ethylene oligomerization induced by the addition of the auxiliary ligand PPh₃ is not well disclosed. We tentatively attribute it to the temporary coordination of PPh₃ with the vacant site formed by the activation of MAO, and thus the active catalytic species are protected. Remarkable induction period was observed during the oligomerization reaction in the presence of PPh₃, which might reflect the coordination of PPh₃ with the vacant site. The PPh₃ group may dissociate again upon approach and coordination of ethylene monomer. Further studies to understand the effects of the auxiliary ligand on the ethylene oligomerization are in progress.

3. Conclusions

A series of bidentate Ni(II) complexes bearing the phosphino-oxazoline ligands were synthesized and fully characterized to reveal their distorted-tetrahedral coordination geometry around the nickel center. Those complexes were found to catalyze ethylene for oligomerization with activities up to 1.18×10^6 g mol⁻¹ (Ni) h⁻¹ (**4d** at 20 atm ethylene pressure), the dimers and trimers being the major products. The ethylene oligomerization activity was found to be affected by the substituents in the ligands framework. Incorporation of steric bulky and electron-donating groups on the carbon atom neighboring the coordinating nitrogen of the oxazoline ring led to the decrease in catalytic activity of ethylene oligomerization, nevertheless, the ethylene oligomerization activity was enhanced with substitution of the groups on phenyl ring attached to the oxazoline. In addition, the oligomerization activity remarkably increased in the presence of 2–4 equiv of PPh₃ as auxiliary ligand.

4. Experimental

4.1. General considerations

All manipulations of air- and/or moisture-sensitive were performed under nitrogen atmosphere using standard Schlenk techniques. Solvents were dried by the literature methods. Methylaluminoxane (MAO) was purchased from Albemarle as a 1.4 M solution in toluene. Other reagents were purchased from Aldrich or Acros Chemicals. ^1H and ^{13}C NMR spectra were recorded on Bruker DMX-300 or 400 MHz instrument using TMS as internal standard. IR spectra were recorded on a Perkin–Elmer system 2000 FT-IR spectrometer. Elemental analysis was carried out using HP-MOD 1106 microanalyzer. GC analysis was performed with a Carlo Erba Strumentazione gas chromatograph equipped with a flame ionization detector and a 30 m (0.25 mm i.d., 0.25 μm film thickness) DM-1 silica capillary column. GC-MS analysis was performed with HP 5890 SERIES II and HP 5971 SERIES mass detector. The yield of oligomer was calculated by referencing with the mass of the used solvent based on the prerequisite that the mass of each fraction is approximately proportional to its integrated areas in the GC trace. Selectivity for linear α -olefin is defined the percentage of α -olefin as (1-olefins/all fractions of olefins) \times 100%.

4.2. Synthesis of halogen-substituted oxazoline compounds **2a–f**

To synthesize the oxazoline compound, various literature methods were reported, including reaction of benzonitrile and amino alcohol in chlorobenzene catalyzed by zinc chloride or using benzoic acid and amino alcohol as starting materials. In comparison, the latter procedure is more controllable and can afford the oxazoline compounds in high yields. Compounds, **2a–2d**, were prepared by the similar procedure, and the synthesis of compound **2a** is selectively as a representative described in detail. 2-Bromobenzoic acid (2.01 g, 0.01 mol) was mixed with thionyl chloride (3.60 g, 0.03 mol), and the mixture was stirred at 40 $^\circ\text{C}$ for 24 h. The excess thionyl chloride was distilled, and the remaining dark oil was further distilled to furnish 2.02 g of the acyl chloride in 92.0% yield. The obtained acyl chloride was dissolved in 20 mL of dichloromethane and dropwise added to a solution of 1-amino-2-propanol (1.38 g, 0.018 mol) in 20 mL of dichloromethane at 0 $^\circ\text{C}$. Then the resulting mixture was stirred at 25 $^\circ\text{C}$ for 2 h, after being concentrated and cooled, the white solid product was filtered and washed with a little dichloromethane to give 2-bromo-*N*-(2-hydroxypropyl)benzamide (2.26 g, 95.0%). Thionyl chloride (3.12 g, 0.026 mol) was dropwise added to a

solution of 2-bromo-*N*-(2-hydroxypropyl)benzamide (2.26 g, 0.088 mol) in 30 mL of toluene at 0 $^\circ\text{C}$. The reaction solution was kept at 80 $^\circ\text{C}$ for 2 h, complete conversion was reached to give the final product, 2.40 g of 2-bromo-*N*-(2-chlorohydroxypropyl)benzamide was obtained in 99.0% yield. The 2-bromo-*N*-(2-chlorohydroxypropyl)benzamide (2.40 g, 0.0087 mol) and NaOH (0.52 g, 0.013 mol) in 40 mL of methanol was refluxed for 5 h. After cooling to room temperature, the resulting solution was treated with brine and extracted with diethyl ether. The organic layer was combined and dried over anhydrous Na_2SO_4 , then the solvent was removed in vacuo, and its residue was purified on the column with silica gel to give the colorless oil, 2-(2-Bromophenyl)-4,5-dihydro-5-methyloxazole (**2a**) (1.61 g, 77.2%). However, the yield of **2a** based on 2-Bromobenzoic acid is 67.2%. ^1H NMR (300 MHz, CDCl_3): δ 7.62–7.70(m, 2H, Ar-H); 7.24–7.37 (m, 2H, Ar-H); 4.82–4.92 (m, 1H, -CH); 4.19 (q, 1H in - CH_2 , $J = 5.9$ Hz); 3.67 (q, 1H in - CH_2 , $J = 5.4$ Hz); 1.45 (d, 3H, - CH_3 , $J = 6.3$ Hz). Anal. Calc. for $\text{C}_{10}\text{H}_{10}\text{BrNO}$: C, 50.02; H, 4.20; N, 5.83. Found: C, 49.89; H, 4.11; N, 5.65%.

2b was obtained as colorless oil in 59.6% yield based on 2-Bromobenzoic acid. ^1H NMR (300 MHz, CDCl_3): δ 7.62–7.69 (m, 2H, Ar-H); 7.27–7.32 (m, 2H, Ar-H); 4.50 (q, 1H in - CH_2 , $J = 7.8$ Hz); 4.27–4.33 (m, 1H, -CH); 4.10 (t, 1H in - CH_2 , $J = 7.8$ Hz); 1.6–1.8 (m, 2H, - CH_2 in ethyl); 1.03 (t, 3H, - CH_3 , $J = 3.8$ Hz). Anal. Calc. for $\text{C}_{11}\text{H}_{12}\text{BrNO}$: C, 51.99; H, 4.76; N, 5.51. Found: C, 52.39; H, 4.78; N, 5.24%. **2c** was obtained as white solid in 71.3% yield based on 2-Bromobenzoic acid. M.p.: 37–39 $^\circ\text{C}$. ^1H NMR (300 MHz, CDCl_3): δ 7.60–7.65 (m, 2H, Ar-H); 7.27–7.33 (m, 2H, Ar-H); 4.14 (s, 2H, - CH_2); 1.42 (s, 6H, - CH_3). Anal. Calc. for $\text{C}_{10}\text{H}_{10}\text{BrNO}$: C, 51.99; H, 4.76; N, 5.51. Found: C, 51.61; H, 4.83; N, 5.39%. **2d** was obtained as colorless oil in 52.7% yield on the base of 2-Bromobenzoic acid. ^1H NMR (300 MHz, CDCl_3): δ 7.53 (d, 1H, Ar-H, $J = 7.8$ Hz); 7.44 (s, 1H, Ar-H); 7.12 (d, 1H, Ar-H, $J = 7.9$ Hz); 4.11 (s, 2H, - CH_2); 2.34 (s, 3H, - CH_3); 1.40 (s, 6H, - CH_3). Anal. Calc. for $\text{C}_{11}\text{H}_{14}\text{BrNO}$: C, 53.75; H, 5.26; N, 5.22. Found: C, 53.72; H, 5.43; N, 5.05%. **2e** was obtained as white solid in 68.4% yield on the base of 2-Bromobenzoic acid. M.p.: 43–45 $^\circ\text{C}$. ^1H NMR (300 MHz, CDCl_3): δ 7.48 (d, 1H, Ar-H, $J = 8.9$ Hz); 7.17 (d, 1H, Ar-H, $J = 3.9$ Hz); 6.84 (dd, 1H, Ar-H, $J_1 = 3.1$ Hz, $J_2 = 8.9$ Hz); 4.13 (s, 2H, - CH_2); 3.81 (s, 3H, - OCH_3); 1.41 (s, 6H, - CH_3). Anal. Calc. for $\text{C}_{11}\text{H}_{14}\text{BrNO}_2$: C, 50.72; H, 4.97; N, 4.93. Found: C, 51.13; H, 5.14; N, 4.78%. **2f** was obtained as viscous colorless oil in 76.4% yield based on 2-Bromobenzoic acid. ^1H NMR (400 MHz, CDCl_3): δ 7.15–7.98 (m, 9H, Ar-H); 5.43 (dd, 1H, -CH, $J = 9.0, 9.0$); 4.80 (t, 1H in - CH_2 , $J = 9.0$); 4.28 (t, 1H in - CH_2 , $J = 9.0$). Anal. Calc. for $\text{C}_{15}\text{H}_{12}\text{FNO}$:

C, 74.67; H, 5.01; N, 5.81. Found: C, 74.50; H, 5.02; N, 5.76%.

4.3. Synthesis of the PHOX ligands

4.3.1. 4,5-Dihydro-5-methyl-2-(2-(diphenylphosphino)-phenyl) oxazole (**3a**)

To a solution of **2a** (0.60 g, 2.5 mmol) in THF (10 mL) was added freshly prepared LiPPh₂ [17] (3.75 mmol, 1.5 equiv) in 10 mL THF solution dropwise at room temperature. The resultant solution was gradually heated to ca. 50 °C and stirred for additional 8 h. All volatiles were removed in vacuo, and the residue was taken up in 30 mL diethyl ether. This solution was washed with degassed water (2 × 10 mL) and then the organic phase was dried over anhydrous Na₂SO₄. Removal of solvent under reduced pressure produced yellow viscous oil. The crude product was purified by flash column chromatography under a nitrogen atmosphere with petroleum ether–ethyl acetate (4:1) as eluent to afford **3a** as white powder in 52.0% yield. M.p.: 92–94 °C. ¹H NMR (300 MHz, CDCl₃): δ 7.84 (dd, 1H, Ar–H, *J*₁ = 3.0 Hz, *J*₂ = 6.0 Hz); 7.31–7.33 (m, 12H, Ar–H); 6.87 (t, 1H, Ar–H, *J* = 5.7); 4.52–4.55 (m, 1H, –CH); 3.87 (q, 1H in –CH₂, *J* = 7.9); 3.34 (q, 1H in –CH₂, *J* = 7.2); 1.12 (d, 3H, –CH₃, *J* = 6.0). Anal. Calc. for C₂₂H₂₀NOP: C, 76.51; H, 6.07; N, 4.01. Found: C, 76.51; H, 5.84; N, 4.06%. ³¹P NMR (CDCl₃): δ –4.58 (s). IR (KBr): 2969; 1661 (*v*_{C=N}); 1472; 1433; 1366, 1329 cm^{–1}.

4.3.2. 4-Ethyl-4,5-dihydro-2-(2-(diphenylphosphino)-phenyl)oxazole (**3b**)

Using the same procedure as for the synthesis of **3a**, **3b** was obtained as a white powder in 41.0% yield. M.p.: 68–70 °C. ¹H NMR (300 MHz, CDCl₃): δ 7.88 (dd, 1H, Ar–H, *J*₁ = 3.4 and 5.8 Hz); 7.30–7.3 (m, 12H, Ar–H); 6.86 (t, 1H, Ar–H, *J* = 3.8); 4.18 (q, 1H in –CH₂); 3.99 (m, 1H, –CH); 3.70 (t, 1H in –CH₂, *J* = 7.9); 1.23–1.38 (m, 2H, –CH₂ in ethyl); 0.79 (t, 3H, –CH₃, *J* = 7.6 Hz). Anal. Calc. for C₂₃H₂₂NOP: C, 76.86; H, 6.17; N, 3.90. Found: C, 76.66; H, 6.48; N, 4.51%. ³¹P NMR (CDCl₃): δ –4.93 (s). IR (KBr): 2960; 1645 (*v*_{C=N}); 1584; 1476; 1433, 1360, 1327 cm^{–1}.

4.3.3. 4,5-Dihydro-4,4-dimethyl-2-(2-(diphenylphosphino)phenyl)oxazole (**3c**)

Using the same procedure as for the synthesis of **3a**, **3c** was obtained as a white powder in 52.1% yield. M.p.: 78–80 °C. ¹H NMR (300 MHz, CDCl₃): δ 7.85 (dd, 1H, Ar–H, *J*₁ = 4.2 and 8.9 Hz); 7.37–7.42 (m, 1H, Ar–H); 7.33 (s, 11H, –Ar–H); 6.79 (t, 1H, Ar–H, *J* = 6.0); 3.73 (s, 2H, –CH₂); 1.05 (s, 6H, –CH₃). Anal. Calc. for C₂₃H₂₂NOP: C, 76.86; H, 6.17; N, 3.90. Found: C, 77.27; H, 6.14; N, 3.87%. ³¹P NMR (CDCl₃): δ –3.92 (s). IR (KBr): 2968; 1646 (*v*_{C=N}); 1585; 1460; 1438, 1351, 1311 cm^{–1}.

4.3.4. 4,5-Dihydro-4,4-dimethyl-2-(4-methyl-2-(diphenylphosphino)phenyl)oxazole (**3d**)

Using the same procedure as for the synthesis of **3a**, **3d** was obtained as a white powder in 43.8% yield. M.p.: 76–78 °C. ¹H NMR (300 MHz, CDCl₃): δ 7.75 (dd, 1H, Ar–H, *J*₁ = 4.1 Hz, *J*₂ = 3.8 Hz); 7.32–7.34 (m, 10H, Ar–H); 7.13 (d, 1H, –Ar–H, *J* = 7.5 Hz); 6.59 (d, 1H, Ar–H, *J* = 4.8); 3.70 (s, 2H, –CH₂); 2.18 (s, 3H, –CH₃). 1.04 (s, 6H, –CH₃). Anal. Calc. for C₂₄H₂₄NOP: C, 76.86; H, 6.17; N, 3.90. Found: C, 77.27; H, 6.14; N, 3.87%. ³¹P NMR (CDCl₃): δ –3.59 (s). IR (KBr): 2967; 1649 (*v*_{C=N}); 1574; 1461; 1435, 1351, 1316 cm^{–1}.

4.3.5. 4,5-Dihydro-2-(5-methoxy-2-(diphenylphosphino)-phenyl)-4,4-dimethyloxazole (**3e**)

Using the same procedure as for the synthesis of **3a** and **3e** was obtained as light yellow viscous oil in 58.8% yield. ¹H NMR (300 MHz, CDCl₃): δ 7.53 (d, 1H, Ar–H, *J* = 6.0 Hz); 7.49 (s, 1H, Ar–H); 7.28–7.32 (m, 9H, –Ar–H); 7.01 (dd, 1H, Ar–H, *J*₁ = 3.0, *J*₂ = 3.0); 6.79 (dd, 1H, Ar–H, *J*₁ = 3.0, *J*₂ = 6.0); 4.10 (s, 2H, –CH₂); 1.39 (s, 6H, –CH₃); 1.09 (s, 3H, –CH₃). ³¹P NMR (CDCl₃): δ –5.92 (s). IR (KBr): 2967; 1649 (*v*_{C=N}); 1590; 1464; 1433, 1352, 1310 cm^{–1}. Repeated elemental analysis measurements for **3e** did not give acceptable results, which might be imputable to the presence of trace of homocoupling compound in **3e**. However, the corresponding complex could be readily purified by recrystallization.

4.3.6. (*S*)-4,5-Dihydro-4-phenyl-2-(2-(diphenylphosphino)phenyl)oxazole (**3f**)

Using the similar procedure for synthesizing LiPPh₂, KPPPh₂ was prepared by the cleavage of PPh₃ with potassium. To the freshly prepared refluxing solution of KPPPh₂ in THF, the fluoro-substituted oxazoline in THF solution was added dropwise. After refluxing for 12 h, the reaction mixture was worked up as described for **3a**. Compound **3f** was separated by flash column chromatography under a nitrogen atmosphere with petroleum ether–ethyl acetate (12:1) as a white solid in 44.5% yield. M.p.: 55–57 °C. ¹H NMR (400 MHz, CDCl₃): δ 6.77–7.96 (m, 19H, Ar–H); 5.70 (t, 1H, –CH, *J* = 9.4); 4.98 (dd, 1H in –CH₂, *J* = 8.3, 8.3); 4.44 (t, 1H in –CH₂, *J* = 8.5). Anal. Calc. for C₂₇H₂₂NOP: C, 79.59; H, 5.44; N, 3.44. Found: C, 79.83; H, 5.39; N, 3.46%. IR (KBr): 3054; 1650 (*v*_{C=N}); 1581; 1466; 1430, 1351, 1307 cm^{–1}.

4.4. Synthesis of the nickel complexes (PHOX)NiBr₂

Complexes **4a–f** were prepared by the similar methods and thus, only one representative procedure is described. The ligand **3a** (0.100 g, 0.29 mmol) and (MEE)NiBr₂ (0.079 g, 0.27 mmol) were added to a Schlenk tube under nitrogen, followed by the addition

of freshly distilled dichloromethane (8 mL) with rapid stirring at room temperature. The solution turned to dark red immediately. The reaction mixture was stirred for 5 h at room temperature, and then concentrated to ca. 4 mL. Hexane (10 mL) was added to precipitate the complex. After filtration and washing with hexane, **4a** was obtained as purple powder in 67.3% yield. IR (KBr): 2979; 1627 ($\nu_{\text{C}=\text{N}}$); 1480; 1435, 1377, 1345 cm^{-1} . Anal. Calc. for $\text{C}_{22}\text{H}_{20}\text{Br}_2\text{NNiOP}$: C, 46.86; H, 3.58; N, 2.48. Found: C, 47.10; H, 3.70; N, 2.46%. **4b** was obtained as orange powder in 84.2% yield. IR (KBr): 2966; 1613 ($\nu_{\text{C}=\text{N}}$); 1565; 1479; 1436, 1376, 1338 cm^{-1} . Anal. Calc. for $\text{C}_{23}\text{H}_{22}\text{Br}_2\text{NNiOP}$: C, 47.80; H, 3.84; N, 2.42. Found: C, 47.46; H, 4.40; N, 2.56%. **4c** was obtained as purple powder in 72.5% yield. IR (KBr): 2966; 1617 ($\nu_{\text{C}=\text{N}}$); 1565; 1480; 1435, 1368, 1319 cm^{-1} . Anal. Calc. for $\text{C}_{23}\text{H}_{22}\text{Br}_2\text{NNiOP} \cdot \text{C}_2\text{H}_2\text{Cl}_2$: C, 43.49; H, 3.65; N, 2.11. Found: C, 42.89; H, 3.29; N, 2.03%. **4d** was obtained as orange powder in 76.5% yield. IR (KBr): 2967; 1613 ($\nu_{\text{C}=\text{N}}$); 1556; 1485; 1459, 1370, 1322 cm^{-1} . Anal. Calc. for $\text{C}_{24}\text{H}_{24}\text{Br}_2\text{NNiOP}$: C, 48.70; H, 4.09; N, 2.37. Found: C, 48.22; H, 4.10; N, 2.31%. **4e** was obtained as purple powder in 69.4% yield. IR (KBr): 2972; 1624 ($\nu_{\text{C}=\text{N}}$); 1588; 1490; 1438, 1368, 1328 cm^{-1} . Anal. Calc. for $\text{C}_{24}\text{H}_{24}\text{Br}_2\text{NNiO}_2\text{P} \cdot \text{CH}_2\text{Cl}_2$: C, 43.34; H, 3.78; N, 2.02. Found: C, 43.74; H, 3.82; N, 2.31%. **4f** was obtained as purple powder in 90.5% yield. IR (KBr): 3055; 1621 ($\nu_{\text{C}=\text{N}}$); 1532; 1435; 1391, 1269, 1120 cm^{-1} . Anal. Calc. for $\text{C}_{27}\text{H}_{22}\text{Br}_2\text{NNiOP}$: C, 51.81; H, 3.54; N, 2.24. Found: C, 51.65; H, 3.78; N, 2.06%.

4.5. Synthesis of the compound 5

Method A: Reaction of 2-(2-bromophenyl)-oxazoline **2f** (0.60 g, 2.5 mmol) with 1.5 equivalent (3.75 mmol) of LiPPh_2 or KPPh_2 in THF solution, using the similar procedure through coupling reaction for the synthesis of **3a**, gave the light yellow oil compound **5** in 39.5% (LiPPh_2) and 42.6% (KPPh_2) yield, respectively, one the base of **2f**. Method B: The 2-(2-bromophenyl)-oxazoline **2f** (0.60 g, 2.5 mmol) reacted with magnesium in 10 mL THF by using the literature method [10a], to the Grignard reagent was added diphenylphosphine chloride (0.71 mL, 3.75 mmol). The mixture was refluxed for 6 h, and the solution was worked up by the similar method for **3a**. Compound **5** was obtained in 60.7% yield. ^1H NMR (400 MHz, CDCl_3): δ 8.05 (dd, 4H, Ar-H, $J_1 = 1.0$ Hz, $J_2 = 1.6$ Hz); 7.29–7.51 (m, 16H, Ar-H); 5.40 (dd, 2H, -CH, $J_1 = 8.2$ Hz, $J_2 = 8.2$ Hz); 4.80 (dd, 2H, $J_1 = 8.4$, $J_2 = 8.4$); 4.28 (t, 2H, -CH₂, $J = 8.3$). ^{13}C NMR (100.61 MHz, CDCl_3): δ 164.72; 142.35; 131.50; 128.72; 128.44; 128.34; 127.59; 127.54; 126.72; 74.85; 70.10. Anal. Calc. for $\text{C}_{30}\text{H}_{24}\text{N}_2\text{O}_2$: C, 81.06; H, 5.44; N, 6.30. Found: C, 80.75; H, 5.97; N, 5.93%. IR (KBr): 3063; 3031, 1720,

1647 ($\nu_{\text{C}=\text{N}}$); 1603; 1580; 1494, 1451, 1357, 1275, 1067, 1026, 974, 951, 760, 697, 540 cm^{-1} .

4.6. General procedure for ethylene oligomerization

4.6.1. Ethylene oligomerization at 1 atm pressure

Complex (5 μmol) was added to a Schlenk type flask under nitrogen. The flask was back-filled three times with N_2 and twice with ethylene, and then charged with toluene and cocatalyst solution in turn under ethylene atmosphere. Under prescribed temperature, the reaction solution was vigorously stirred under 1 atm ethylene for the desired period of time. The oligomerization reaction was quenched by the addition 60 mL 10% HCl solution. About 1 mL of organic solution was dried by anhydrous Na_2SO_4 for GC analysis. No polyethylene formation was observed after pouring the remained solution into 100 mL of ethanol.

4.6.2. Ethylene oligomerization at 20 atm pressure

High-pressure ethylene polymerization was performed in a stainless steel autoclave (1 L capacity) equipped with gas ballast through a solenoid valve for continuous feeding of ethylene at constant pressure. One hundred and thirty seven milliliters of toluene containing the catalyst precursor was transferred to the fully dried reactor under nitrogen atmosphere, and then 13 mL of MAO in toluene solution was then injected into the reactor using a syringe. As the prescribed temperature was reached, the reactor was pressurized to the 20 atm. After stirring for 30 min, the reaction was quenched and worked up using the same method as described above for 1 atm reaction.

4.7. X-ray crystallographic studies

The single-crystal X-ray diffraction for complex **4c** was carried out on a Rigaku RAXIS Rapid IP diffractometer with graphite monochromated Mo $\text{K}\alpha$ radiation ($\lambda = 0.71073$ Å) at 173(2) K. Intensity data of complex **4d** and **4e** were collected on a Bruker SMART 1000 CCD diffractometer with graphite monochromated Mo $\text{K}\alpha$ radiation ($\lambda = 0.71073$ Å) at 293(2) K. Cell parameters were obtained by global refinement of the positions of all collected reflections. Intensities were corrected for Lorentz and polarization effects and empirical absorption. The structures were solved by direct methods and refined by full-matrix least-squares on F^2 . All non-hydrogen atoms were refined anisotropically. All hydrogen atoms were placed in a calculated position. Structure solution and refinement were performed by using the SHELXL-97 Package. Crystal data and processing parameters for complexes **4c–4e** are summarized in Table 5. Crystallographic data of complexes **4c–4e** were deposited with the Cambridge Crystallographic Data Centre, CCDC 268442, 268443

Table 5
Crystallographic data and refinement for **4c** · CH₂Cl₂, **4d** and **4e**

	4c · CH ₂ Cl ₂	4d	4e
Formula	C ₂₃ H ₂₂ Br ₂ NNiOP · CH ₂ Cl ₂	C ₂₄ H ₂₄ Br ₂ NNiOP	C ₂₄ H ₂₄ Br ₂ NNiO ₂ P
Fw	660.83	591.94	607.94
Cryst syst.	Monoclinic	Monoclinic	Monoclinic
Space group	<i>P</i> 2(1)/ <i>c</i>	<i>P</i> 2(1)/ <i>c</i>	<i>P</i> 2(1)/ <i>c</i>
<i>a</i> (Å)	9.0424(18)	9.3188(11)	8.8285(13)
<i>b</i> (Å)	15.728(3)	26.555(3)	20.860(3)
<i>c</i> (Å)	18.908(4)	9.8290(12)	14.168(2)
α (°)	90	90	90
β (°)	91.39(3)	95.831(2)	104.201(2)
γ (°)	90	90	90
<i>V</i> (Å ³)	2688.3(9)	2419.7(5)	2529.6(6)
<i>Z</i>	4	4	4
<i>D</i> _{calcd.} (g · cm ⁻³)	1.633	1.625	1.596
Absorption coefficient, μ , (mm ⁻¹)	3.969	4.186	4.009
<i>F</i> (000)	1312	1184	1216
θ range, (deg)	2.59–27.45	1.53–26.05	1.78–26.03
Number of data collected	11,159	13,528	14,119
Number of unique data	6018	4766	4980
<i>R</i>	0.0370	0.0272	0.0332
<i>R</i> _w	0.1119	0.0360	0.0496
Goodness-of-fit	0.623	1.029	1.032

and 268444, respectively. Copies of this information may be obtained free of charge from CCDC, 12 Union Road, Cambridge, CB2 1 EZ, UK (fax: +44 1223 336033; e-mail: deposit@ccdc.cam.ac.uk or <http://www.ccd.cam.ac.uk>).

Acknowledgement

The project supported by NSFC No.20272062 and 20473099. This work was partly completed in Polymer Chemistry Laboratory, Chinese Academy of Sciences and China Petro-Chemical Corporation.

References

- [1] D. Vogt, in: B. Cornils, W.A. Herrmann (Eds.), *Applied Homogeneous with Organometallic Compounds*, vol. 1, VCH, New York, 1996, pp. 245–258.
- [2] (a) W. Keim, F.H. Kowaldt, R. Goddard, C. Kruger, *Angew. Chem., Int. Ed. Engl.* 17 (1978) 466;
(b) W. Keim, A. Behr, B. Limbacher, C. Kruger, *Angew. Chem., Int. Ed. Engl.* 22 (1983) 503;
(c) W. Keim, A. Behr, G. Kraus, *J. Organomet. Chem.* 251 (1983) 377;
(d) U. Klabunde, S.D. Itten, *J. Mol. Catal.* 41 (1987) 123;
(e) P. Grenouillet, D. Neibecker, I. Tkatchenko, *J. Organomet. Chem.* 243 (1983) 213.
- [3] L.K. Johnson, C.M. Killian, M. Brookhart, *J. Am. Chem. Soc.* 117 (1995) 6414.
- [4] (a) J. Feldman, S.J. McLain, A. Parthasarathy, W.J. Marshall, J.C. Calabrese, S.D. Arthur, *Organometallics* 16 (1997) 1514;
(b) M. Helldörfer, J. Backhaus, W. Milius, H.G. Alt, *J. Mol. Catal. A.* 193 (2003) 59;
(c) D.H. Camacho, E.V. Salo, J.W. Ziller, Z. Guan, *Angew. Chem., Int. Ed. Engl.* 43 (2004) 1821.
- [5] (a) S. Plentz-Meneghetti, P.J. Lutz, J. Kress, *Organometallics* 18 (1999) 2734;
(b) T.V. Laine, K. Lappalainen, J. Liimatta, E. Aitola, B. Löfgren, M. Leskelä, *Macromol. Rapid. Commun.* 20 (1999) 487;
(c) W.-H. Sun, X. Tang, T. Gao, B. Wu, W. Zhang, H. Ma, *Organometallics* 23 (2004) 5037;
(d) X. Tang, W.-H. Sun, T. Gao, J. Hou, J. Chen, W. Chen, *J. Organomet. Chem.* 690 (2005) 1570.
- [6] (a) C. Wang, S. Friedrich, T.R. Younkin, R.T. Li, R.H. Grubbs, D.A. Bansleben, M.W. Day, *Organometallics* 17 (1998) 3149;
(b) T.R. Younkin, E.F. Connor, J.I. Henderson, S.K. Friedrich, R.H. Grubbs, D.A. Bansleben, *Science* 287 (2000) 460;
(c) L. Wang, W.-H. Sun, L. Han, Z. Li, Y. Hu, C. He, C. Yan, *J. Organomet. Chem.* 650 (2002) 59.
- [7] (a) O. Daugulis, M. Brookhart, *Organometallics* 21 (2002) 5926;
(b) W.-H. Sun, Z. Li, H. Hu, B. Wu, H. Yang, N. Zhu, X. Leng, H. Wang, *New J. Chem.* 26 (2002) 1474;
(c) O. Daugulis, M. Brookhart, P.S. White, *Organometallics* 21 (2002) 5935;
(d) F. Speiser, P. Braunstein, L. Saussine, R. Welter, *Organometallics* 23 (2004) 2613;
(e) F. Speiser, P. Braunstein, L. Saussine, *Organometallics* 23 (2004) 2625;
(f) F. Speiser, P. Braunstein, L. Saussine, *Organometallics* 23 (2004) 2633;
(g) J. Heinicke, M. Köhler, N. Peulecke, M.K. Kindermann, W. Keim, M. Köckerling, *Organometallics* 24 (2005) 344.
- [8] (a) S.D. Ittel, L.K. Johnson, M. Brookhart, *Chem. Rev.* 100 (2000) 1169;
(b) V.C. Gibson, S.K. Spitzmesser, *Chem. Rev.* 103 (2003) 283.
- [9] H.A. McManus, P.J. Guiry, *Chem. Rev.* 104 (2004) 4151, and references cited therein.

- [10] (a) A.I. Meyers, D.S. Temple, D. Haidukewych, E.D. Mihelich, *J. Org. Chem.* 39 (1974) 2787;
(b) J. Spinz, G. Helmchen, *Tetrahedron Lett.* 34 (1993) 1769;
(c) M. Peer, J.C. de Long, M. Kiefer, T. Langer, H. Rieck, H. Schell, P. Sennhenn, J. Sprinz, H. Steinhagen, B. Wiese, G. Helmchen, *Tetrahedron* 52 (1996) 7583.
- [11] J.V. Allen, G.J. Dawson, C.G. Frost, J.M.J. Williams, *Tetrahedron* 50 (1994) 799.
- [12] G.C. Lloyd-Jones, C.P. Butts, *Tetrahedron* 54 (1998) 901.
- [13] L.P. Spencer, R. Altwer, P. Wei, L. Gelmini, J. Gauld, D.W. Stephan, *Organometallics* 22 (2003) 3841.
- [14] J.M. Malinoski, M. Brookhart, *Organometallics* 22 (2003) 5324.
- [15] M.S.W. Chan, L. Deng, T. Ziegler, *Organometallics* 19 (2000) 2741.
- [16] J.C. Jenkins, M. Brookhart, *Organometallics* 22 (2003) 250.
- [17] K.Z. Sommer, *Anorg. Allg. Chem.* 376 (1970) 37.